Biomass and Bioenergy 186 (2024) 107260

Contents lists available at ScienceDirect

Biomass and Bioenergy

journal homepage: www.elsevier.com/locate/biombioe

Determination of biomass drying speed using neural networks

Borja Velázquez Martí [a,*], Alfredo Bonini Neto [b], Daniel Nuñez Retana [a], Artemio Carrillo Parra [c], Sebastian Guerrero-Luzuriaga [d]

[a] Departamento de Ingeniería Rural y Agroalimentaria, Universitat Politècnica de València, Camino de Vera s/n, 46022, Valencia, Spain
[b] Department of Biosystems Engineering, School of Sciences and Engineering, São Paulo State University (Unesp), Tupã, 17602-496, Brazil
[c] Institute of Silviculture and Wood Industry, Juárez University of the State of Durango, Boulevard del Guadiana 501, Ciudad Universitaria, Research Tower, 34120, Durango, Durango, Mexico
[d] Carrera de Agroindustria, Universidad Nacional de Chimborazo, Km 1 ½ Vía Guano Campus "Edison Riera", 060107, Riobamba, Ecuador

ARTICLE INFO

Keywords:
Neuronal networks applications
Biomass drying
Biomass processing
Drying kinetics

ABSTRACT

The difficulty of measuring the drying rate of biomass under hot air convection conditions due to the influence of multiple factors, such as environmental conditions and material properties; and the problems associated with the variability of desiccation curves under changing conditions makes the use of mass transfer models based on diffusion and convection generally quite inaccurate. The research proposes the use of neural networks to determine the average drying speed (g removed water in unit of biomass material (kg) in unit time (s)), highlighting its ability to handle complex and variable data, as well as its adaptability and robustness. After 62 iterations, the R^2 of the training process reached values of 0.93. Subsequent validation provided an R^2 of 0.88. The mean square error was less than 10^{-3} g dryed water kg^{-1} biomass s^{-1}. Traditional mass transfer models applied to drying processes were compared with experimental data. It has been proven that the values of the convection coefficient in mass transfer are overestimated when obtained from the Sherwood number. Values of this coefficient applied to wood are 30 times lower due to capillary phenomena and electrostatic forces between the material and the water particles.

1. Introduction

Measuring the drying rate of biomass in a hot air convection process can be a challenging task due to the influence of multiple factors that affect this process. Some of the difficulties associated with measuring drying rate include environmental conditions such as temperature, humidity, and air circulation speed [1]. These variables are difficult to control and can change during the drying process, complicating accurate measurement [2,3]. Furthermore, different materials have different drying properties. The composition of the material, its thickness, the presence of solvents and other intrinsic factors can affect the rate of evaporation of the liquid and, therefore, the rate of drying. The shape and surface of the material being dried can also affect. Rough or uneven surfaces may have areas that dry more slowly than others [4]. On the other hand, in some cases, chemical or physical interactions between the material and the drying medium can influence the drying rate. For example, the formation of a crust on the surface can affect the evaporation of liquid.

A fairly common trend in scientific literature has been to carry out experiments from which curves are drawn that relate humidity to time when the process is carried out under fixed conditions. However, when conditions change, the curves representing desiccation also vary [5,6]. Therefore, the impossibility of making infinite curves prevents an accurate prediction of the drying rate for changing conditions.

An alternative to the use of empirical desiccation curves is the use of mass transfer models, which are based on diffusion phenomena and mass transfer by convection [5,7].

Diffusion transfer phenomena use equations where there is a proportionality between the mass transfer rate and the particle concentration gradient between two specific points in a system [8]. The proportionality constant in a diffusion process is the diffusion coefficient defined in Fick's law, also called diffusivity (D_g) [8]. Convection transfer phenomena use equations where there is a proportionality between the mass transfer rate and the difference in particle concentration between two specific points in a system. In a convection mass transfer process, the proportionality constant is defined as convection mass transfer

* Corresponding author.
E-mail address: borvemar@dmta.upv.es (B. Velázquez Martí).

https://doi.org/10.1016/j.biombioe.2024.107260
Received 12 February 2024; Received in revised form 20 April 2024; Accepted 26 May 2024
Available online 30 May 2024

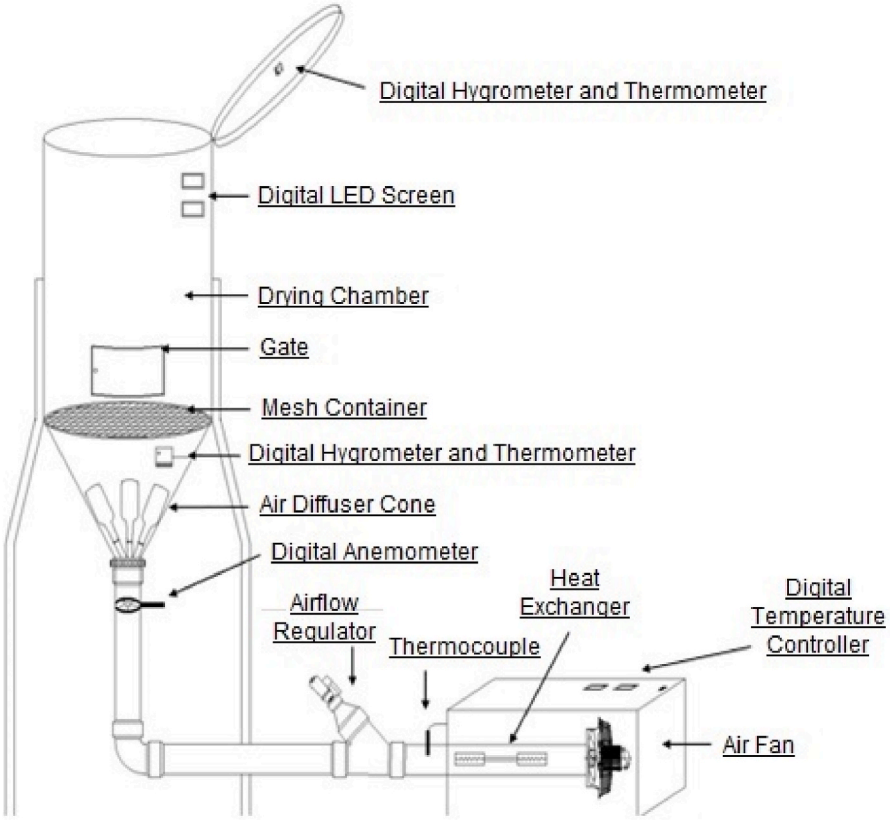

Fig. 1. Experimental biomass dryer.

coefficient (h_m) [7,8].

The problem with using these mass transfer models lies in the difficulty of measuring accurately the diffusivity (D_g) and the mass transfer coefficient (h_m) [5,9]. However, traditional mass transfer models come with their set of constraints. While correlation equations to obtain the Sherwood Number and subsequently calculating the convection mass transfer coefficient, along with the Fick equation for determining diffusion drying rates, perform admirably in liquid sheets, their efficacy diminishes when dealing with liquid particles confined within pores experiencing capillary or electrostatic forces. In such scenarios, the predictions of particle flow removal from the solid can deviate from those anticipated by mass transfer models [10,11].

On the other hand, the moisture content of the piece in the drying process may not remain uniform throughout the mass. It will depend on the dimensions of the pieces to be dried and the internal diffusivity [11]. When the particle size is excessively large, or in the case of blocks and boards, only the surface of the biomass dries by convection, while as the thickness increases, the air does not reach the deepest parts of the pores. Then their particles only move through them by diffusion [12,13]. Therefore, if the drying speed is analyzed on a dry basis with respect to the moisture content of the biomass, a variation of this depending on the moisture content is detected. When the moisture content of the biomass is high, the drying rate is constant, but below a certain value, called critical, the drying rate decreases [14]. The evaluation of the consideration of a uniform drying process in a piece depends on the Biot number in mass transfer (Bi_m). The Biot number in mass transfer is the ratio of the resistance to internal mobility of water particles of a body with respect to mass convection at the surface. Therefore, a small Biot number represents little resistance to internal diffusion of the mass and, therefore, small moisture gradients within the body. To consider the drying process uniform throughout the mass of a piece, it is conventionally verified that que $Bi_m < 0.5$. (Note: in heat transfer it is considered zero dimensional when Bi < 0.1)

$$Bi_m = \frac{h_m \cdot L_b}{D_g} \quad (1)$$

Experimentally, different drying kinetics have been observed in configurations where the convective air current circulates over the surface of a mass, or crosses a network of particles in an ascending or descending direction [15].

Determining the average drying rate using neural networks can offer several advantages compared to more traditional approaches or simplified modeling. On the one hand, neural networks are capable of learning non-linear relationships between input variables and output variables. This is crucial when the interactions between different factors do not follow simple linear patterns, which is common in complex processes such as drying [16]. Drying processes can be affected by a wide variety of environmental variables and material properties. Neural networks can adapt to the complexity of this data and capture patterns not evident to the naked eye. As more data becomes available to train the neural network, its predictive ability tends to improve. Neural networks are relatively robust in the presence of noisy or incomplete data. They can handle unstructured information and learn patterns even when there is variability in the data. You can include a variety of variables as input to the neural network, such as air temperature, air moisture content, type of material, etc. [17–19]. This allows for more complete and accurate modeling of the drying process by considering multiple factors simultaneously.

Although Artificial Neuronal Networks (ANN) are powerful tools in many contexts, they also present certain drawbacks and challenges that are important to take into account when analyzing drying processes. RNAs tend to need large and representative data sets to be properly trained [20]. This means that the number of drying processes must be large for a large set of materials. The quality and quantity of data available for this study could limit its effectiveness. With the use of a reduced number of data there is a risk that an RNA will adjust too much

to the training data and cannot generalize well to new data, which leads to poor performance in practical situations. On the other hand, unlike some traditional methods, such as linear regressions, RNA can be difficult to interpret. This can make it difficult to understand how and why an RNA reaches certain conclusions.

The RNA may be sensitive to the quality of the input data, including errors or errors in the data. An outlayer is not easily detected. This can significantly affect your performance and precision.

Despite these drawbacks, the ANN continues to be a valuable tool in a wide range of applications, and many of these challenges can be mitigated with appropriate design practices and advanced automatic learning techniques. The choice of modeling technique will depend on the specific nature of the problem and the requirements of the system in question [21]. The main objective of the research presented in this article is to develop a predictive model that can accurately estimate the drying speed of materials based on various input variables through the use of neural networks, as well as compare the results with models based on data transfer. Traditional convection dough.

2. Materials and methods

2.1. Material under study

For the drying tests, logs of the genus *Pinus* spp. randomly selected samples obtained from a sawmill in the municipality of Durango (Mexico). Subsequently, they were cut and chipped using a crusher until they had a P16*S* grain size *P16S* (3.15 mm $< P \leq$ 16 mm) in accordance with the UNE-EN 17225-4 standard [22]. So that they did not lose moisture, the chips obtained were kept stored in a controlled environment at 20 °C and 80 % relative humidity. Prior to the drying tests, the initial moisture content was determined in accordance with the UNE-EN 18134-3 standard [23] which reached 36.23 % with a standard deviation 7.39 %. The bulk wet density was 321.21 kg/m^3 with a standard deviation 18.29 kg/m^3. Percentage of bark in the wet chips was 1.352 % with a standard deviation of 0.35 %.

2.2. Experimental device

Fig. 1 shows the design of the experimental dryer, which consists of a vertical cylinder. Inside, there is a column of chips through which an ascending current of hot air circulates to carry out the drying process. The vertical displacement of hot air facilitates the removal of humid air through the top of the device. The drying cylinder has a diameter of 60 cm and a height of 89.4 cm. The feeder cone placed at the bottom of the cylinder has a lower diameter of 7.10 cm with a height of 55 cm. The feed pipe has a diameter of 7.10 cm and 60 cm of horizontal length before the elbow, and 18.5 cm of vertical length after the elbow to the entrance of the cone. The air is propelled by a fan located in a supply pipe. Subsequently, the air is heated by resistors whose variable power allows the temperature to be adjusted. A valve at the fan outlet regulates the air flow to the drying column. This heated air advances towards a diffuser cone, responsible for uniformly distributing the air throughout the cylinder section. After the diffuser cone, there is a mesh that acts as a retainer for the chips, preventing them from falling into the air supply pipe and preventing possible technical problems such as blockages or ignition of the chips. The system has air speed, air temperature and air humidity sensors located in the diffuser cone (before contact with the chips) and at the dryer outlet. Sensor locations are depicted in Fig. 1.

2.3. Measurement procedure

Three boxes made of fine wires were filled with chips. These boxes were placed in the middle of the column of chips during the drying process. Every 10 min for a period of 2.5–8 h the dryer was stopped, the boxes were removed, and weighed on a scale. The materials inside the box were previously sieved to avoid the loss of excessively small particles between two consecutive weight measurements. These boxes had measurements of 13.5 × 6.5 × 5.0 cm.

Table 1
Levels of the factors evaluated in each experiment.

Air Velocity (m/s)		Temperature (°C)		Height (cm)	
v_1	6.93–8.46	T_1	40.10–48.84	H_1	3
v_2	8.46–9.99	T_2	48.84–57.58	H_2	6
		T_3	57.58–66.32		

The difference in weight between two consecutive measurements represents the water evaporated every 10 min. The amount of water evaporated per kilogram of dry biomass per second represents the relative drying speed.

After the drying process the moisture content of the chips inside boxes was measured with the UNE-EN 18134-3 standard [23]. This measurement allowed knowing the dried mass of these chips, and therefore the moisture content in each measurement during the drying process.

To evaluate the drying process by convection with hot air, 12 treatments were evaluated, each treatment with 18 repetitions, with a total of 216 experiments. Two levels of air velocity $\{v_1, v_2\}$, three levels of temperature $\{T_1, T_2, T_3\}$ and two levels of chip column height $\{H_1, H_2\}$. were combined. Table 1 presents the characteristic values of each level used in the study.

The speed, temperature and humidity sensors made it possible to determine the air conditions before and after passing through the desiccation column.

2.4. Characterization of the drying process

6 variables have been determined that characterize the drying speed.

- Mean relative drying speed ($\overline{\dot{m}_w}$). It is defined as the average mass of water that is removed from the chips per kg of dry solid mass and unit of time (g of water s^{-1} kg of dry chip^{-1}). It is calculated by equation (2), where m_i is the initial mass of the chips in g; m_f is the final mass of the chips in g; t is the time of the drying process in s; m_{dry} is the mass of the dry chips in kg.

$$\overline{\dot{m}_w} = \frac{m_i - m_f}{t \bullet m_{seca}} \tag{2}$$

- Mean absolute drying speed ($\overline{\dot{m}_s}$). It is defined as the average mass of water that is removed from the chips per unit of time (g of water s^{-1}). It is calculated by equation (3).

$$\overline{\dot{m}_s} = \frac{m_i - m_f}{t} \tag{3}$$

- Instantaneous relative drying speed ($\dot{m}_w$). It is defined as the mass of water that is being removed from the chips at a given instant per kg of dry solid mass (g of water s^{-1} kg of dry chip^{-1}). It is calculated by equation (4), where m_1 is the mass of the chips at time t_1 in g; m_2 is the mass of the chips at time t_2; m_{dry} is the mass of the dry chips in kg.

$$\dot{m}_w = \frac{m_1 - m_2}{(t_2 - t_1) \bullet m_{seca}} \tag{4}$$

- Instantaneous absolute drying speed ($\dot{m}_s$). It is defined as the mass of water that is being removed from the chips at a given instant (g of water s^{-1}). It is calculated by equation (5).

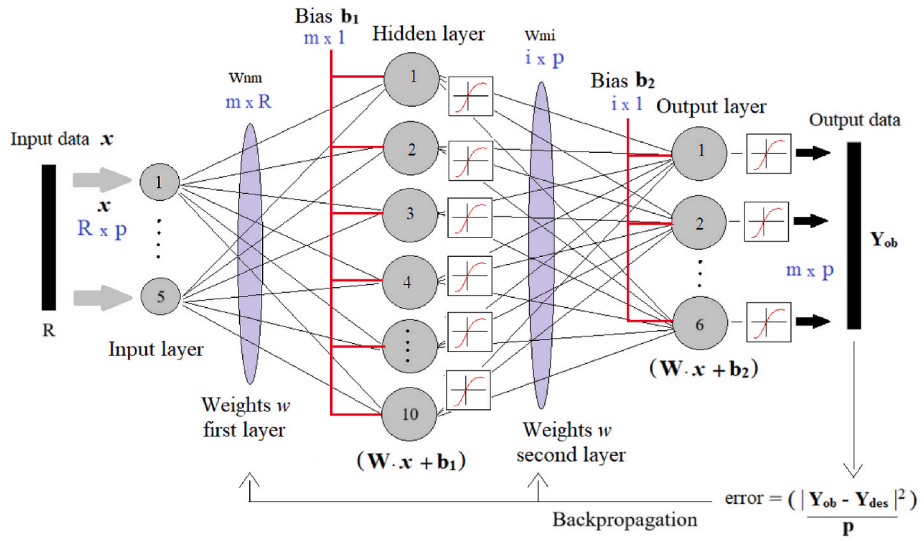

Fig. 2. Artificial neural network – ANN (feedforward) used in this work to estimate the drying speed.

$$\dot{m}_s = \frac{m_1 - m_2}{t_2 - t_1} \tag{5}$$

- Convection mass transfer coefficient h_m, such that it meets equation (6).

$$\dot{m}_s = h_m \cdot A \cdot \rho_{aire} \cdot (\omega_{sat\ air} - \omega_{air}) \tag{6}$$

Where h_m is de coefficient of mass transfer, A is the transfer area, ρ_{aire} is de air density at treatment temperature, $\omega_{sat\ air}$ is air absolute humidity in saturation at treatment temperature, ω_{air} is air absolute humidity.

It was evaluated how the instantaneous drying speeds (relative and absolute) and the mass transfer coefficient by convection are modified as a function of the moisture content of the chips, obtaining the slopes of the corresponding curves $\frac{d\dot{m}_w}{d\omega}$, $\frac{d\dot{m}_s}{d\omega}$ y $\frac{dh_m}{d\omega}$.

The experimental convection mass transfer coefficient h_m was compared with that obtained theoretically using equation (7), where *Sh* is the Sherwood number, L_c the characteristic length and D_w the mass diffusivity at the solid-air interface.

$$h_m = \frac{Sh \cdot L_c}{D_w} \tag{7}$$

2.5. Design and modeling by neural networks

The Artificial Neural Network (ANN) used in this study, as shown in Fig. 2, was the Multilayer Perceptron (MLP) composed of five neurons in the input layer r = 5 (air velocity (m/s), air temperature (°C), relative humidity (%), chip column height (cm) and average sliver length (m)), then ten neurons in the intermediate layer (m = 10) and six neurons in the output layer (i = 6), representing the drying speed, as average relative drying speed (g/s kg) ($\overline{\dot{m}_w}$), average absolute drying speed (g/s) ($\overline{\dot{m}_s}$), average moisture content variation (%/s) ($\overline{\dot{\omega}}$), slope of the variation of the average relative drying speed ($\frac{d\dot{m}_w}{d\omega}$), slope of the variation of the average absolute drying speed ($\frac{d\dot{m}_s}{d\omega}$) and slope of moisture content variation ($\frac{d\dot{\omega}}{d\omega}$).

The activation functions for the outputs of both layers were the hyperbolic tangent, given by equation (8):

$$f(u) = \frac{(1 - e^{-\lambda u})}{(1 + e^{-\lambda u})} \tag{8}$$

where λ is an arbitrary constant and corresponds to the slope of the curve, while the platform used for the computational implementation of the ANN and obtaining the results was MATLAB [24].

Of the 207 samples used in this work, 80 % were used in training and 20 % for validation (samples that were not part of the training). The validation process was carried out last year using two strategies. On the one hand, new samples were introduced into the calculation system and the result obtained was compared with experimental data using techniques in paired samples based on the student. On the other hand, cross-validation was carried out.

All inputs were normalized data obtained through equation (9) to concentrate the values between 0 and 1, facilitating the training of network and the choice the transfer function (hyperbolic tangent), resulting in a much smaller error in the training process compared to non-normalized (conventional) data. Finally, these data are returned to real values for better interpretation in the results and discussion.

$$Y_{des}normalized = \frac{Y_{des}}{\max(Y_{des})} \tag{9}$$

Neural networks that use backpropagation algorithm, as well as many other types of artificial neural networks, can be seen as difficult to interpret systems, in which it is almost unknown why the network reaches a certain result, since the models do not present justifications for their answers [19]. Therefore, it may be noted that a different value will always be obtained for each time the network is retrained [19]. Based on this, it was developed a procedure to initialize the training program multiple times, using different configurations, both for the number of hidden layers and the number of neurons (varying in increments of 5 neurons), as well as for the proportions of training and validation samples (varying in increments of 5 %). After repeating the process *n* times, the best result obtained was stored, corresponding to the most effective configuration (optimal number of hidden layers and neurons) that resulted in the highest accuracy percentage in the validation phase. In the study in question, the most successful configuration consisted of one hidden layer with 10 neurons, with 20 % of the samples reserved for validation.

3. Results and discussion

Among the 207 samples, 80 % (166 samples) were randomly selected for the training process, while the remaining 20 % (41 samples) were reserved for validation. Network training was carried out over a 20-s interval, during which 62 iterations occurred. In Fig. 3(a), the training

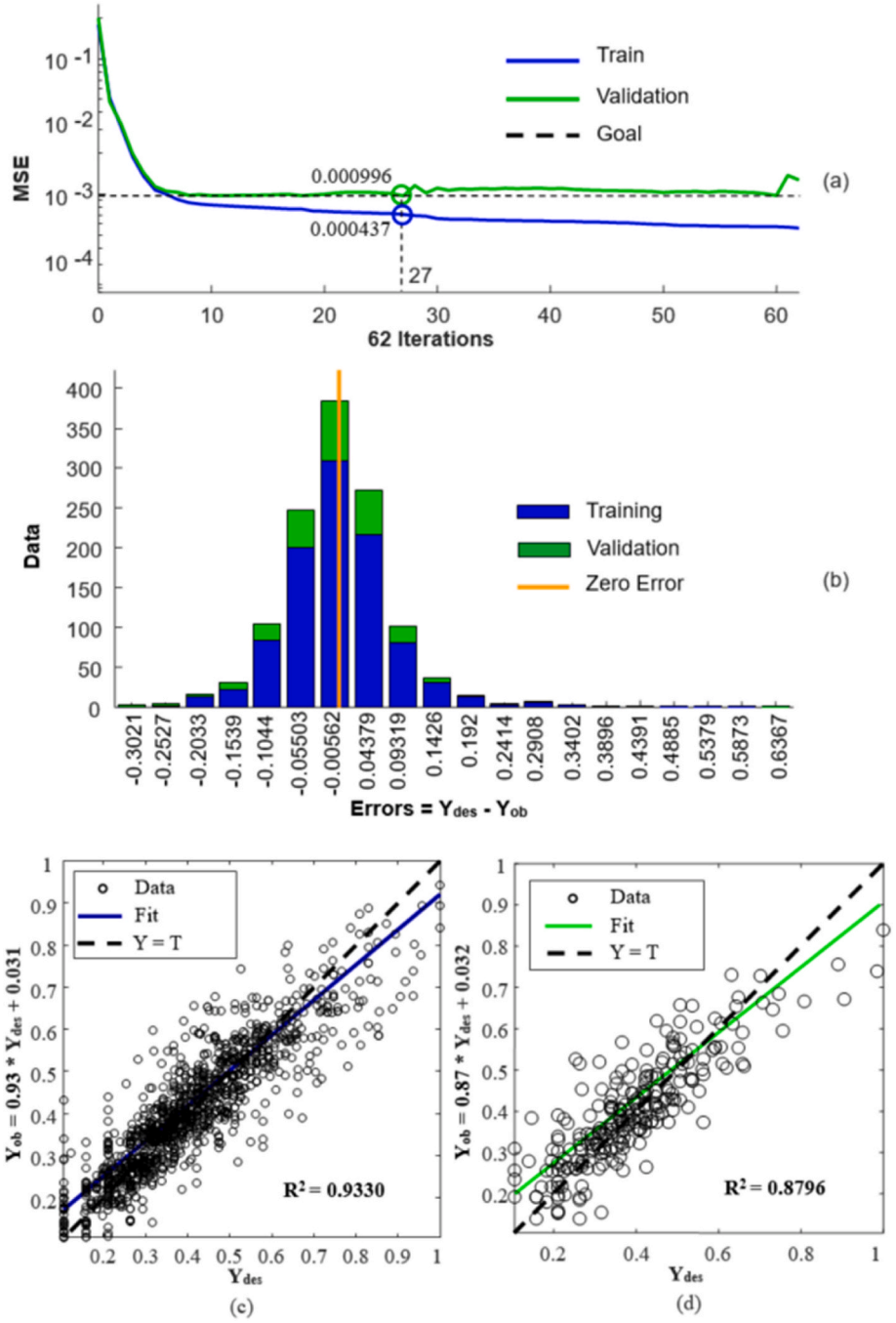

Fig. 3. Training and validation performance, (a) mean square error (MSE), (b) histogram with respect to error ($\mathbf{Y_{des}}$ - $\mathbf{Y_{ob}}$), (c) correlation between obtained ($\mathbf{Y_{ob}}$) and desired ($\mathbf{Y_{des}}$) output in training, (c) correlation between obtained ($\mathbf{Y_{ob}}$) and desired ($\mathbf{Y_{des}}$) output in validation.

and validation performances in relation to the mean squared error (MSE) are presented. It is noteworthy that in the twenty-seventh iteration, the best values were achieved for both validation (MSE = 0.000996) and training (MSE = 0.000437), both below the specified limit of 10^{-3}.

Fig. 3(b) displays a histogram of the data from the two phases of the network relative to zero for the error ($|\mathbf{Y_{ob}} - \mathbf{Y_{des}}|$). It can be observed that the majority of the data displayed errors close to zero. Regarding Fig. 3(c) and (d), they provide a correlation analysis for the training and validation of the network, presenting the correlations between the obtained output ($\mathbf{Y_{ob}}$) and the desired output ($\mathbf{Y_{des}}$), respectively. The R^2 values obtained were in accordance with expectations for both analyzes (0.9330 and 0.8796), indicating that 93 % and 87 % of the vector

Table 2
Values specified and achieved ($\mathbf{Y_{ob}}$) in the network training and validation compared with output ($\mathbf{Y_{des}}$).

	Specified values	Values achieved
Iterations	1000	62
Time CPU (seconds)	20	[a] 20
Training Performance (MSE)	0.001	[a] 0.000437
Training Correlation R^2	1.0	0.9330
Validation Performance (MSE)	0.001	[a] 0.000996
Validation Correlation R^2	1.0	0.8796

[a] Achieved criterion.

Table 3
Weights of the connections between the neurons of the input layer and the hidden layer (w_{nm}).

		Neurons hidden layer									
		m_1	m_2	m_3	m_4	m_5	m_6	m_7	m_8	m_9	m_{10}
Neurons input layer	$\mathbf{n_1}$	1.2768	1.7456	0.4660	−1.1092	−0.6945	0.4495	−0.4824	−1.9147	1.7490	−0.8471
	$\mathbf{n_2}$	1.0022	0.0455	0.4510	0.4879	−0.4301	0.2325	1.7586	−0.3180	−1.3766	−0.5417
	$\mathbf{n_3}$	−1.0777	−0.3473	−0.9316	−0.3526	−1.1059	1.1293	0.2513	0.6214	−0.7482	0.9401
	$\mathbf{n_4}$	1.4253	−0.8900	0.7275	1.1097	1.7185	−1.5020	1.1522	0.8310	1.3147	0.6580
	$\mathbf{n_5}$	−0.6526	1.1782	2.3171	0.4243	3.6031	−0.3044	−1.4225	1.0701	−0.3827	0.4119

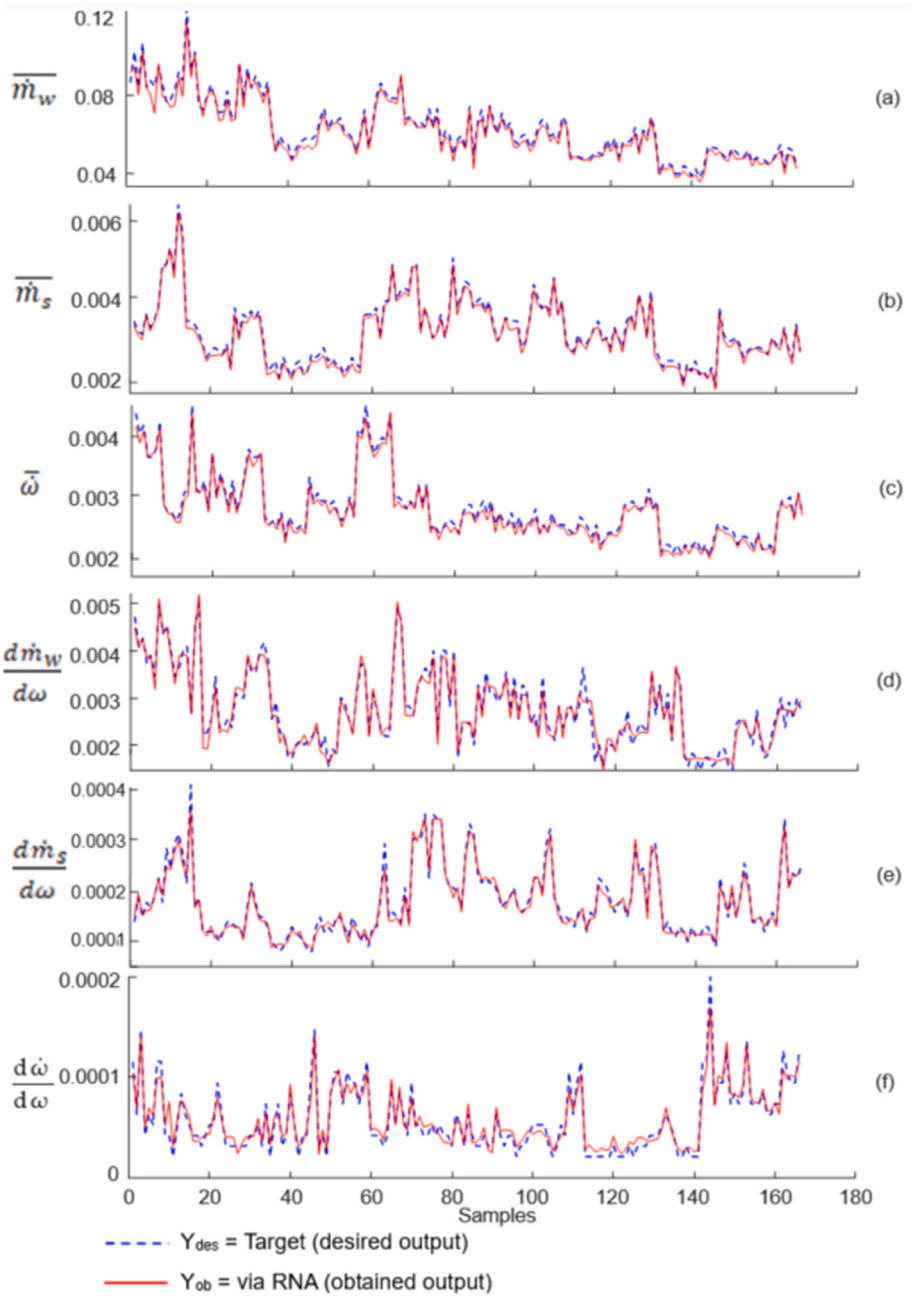

Fig. 4. Training phase, desired output $\mathbf{Y_{des}}$ versus obtained output using neural networks $\mathbf{Y_{ob}}$ de drying speed, (a) average relative drying speed (g/s kg) ($\overline{\dot{m}_w}$), (b) average absolute drying speed (g/s) ($\overline{\dot{m}_s}$), (c) average moisture content variation (%/s) ($\overline{\dot{\omega}}$), (d) slope of the variation of theaverage relative drying speed ($\frac{d\dot{m}_w}{d\omega}$), (e) slope of the variation of theaverage absolute drying speed ($\frac{d\dot{m}_s}{d\omega}$), (f) slope of moisture content variation ($\frac{d\dot{\omega}}{d\omega}$).

generated ($\mathbf{Y_{ob}}$) by the Artificial Neural Network (ANN) are explained by the desired variables ($\mathbf{Y_{des}}$). Table 2 substantiates these results, presenting the specified values for the training and validation phases of the ANN, along with the values achieved by it (see Table 3).

Fig. 4 displays the results, comprising a comparison between the outputs obtained by the ANN ($\mathbf{Y_{ob}}$) and the desired outputs derived from

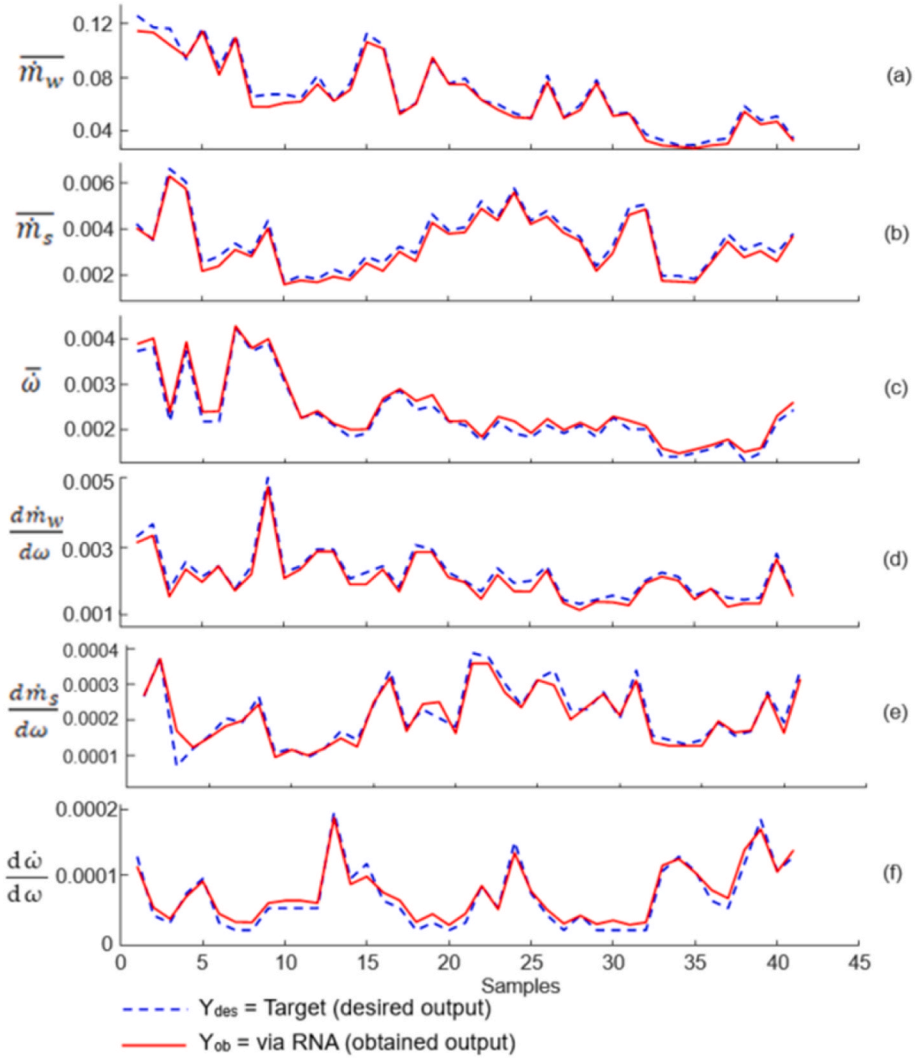

Fig. 5. Validation phase (samples that were not part of the training phase), desired output $\mathbf{Y_{des}}$ versus obtained output using neural networks $\mathbf{Y_{ob}}$ of drying speed, (a) average relative drying speed (g/s kg) ($\overline{\dot{m}_w}$), (b) average absolute drying speed (g/s) ($\overline{\dot{m}_s}$), (c) average moisture content variation (%/s) ($\bar{\omega}$), (d) slope of the variation of the average relative drying speed ($\frac{d\dot{m}_w}{d\omega}$), (e) slope of the variation of the average absolute drying speed ($\frac{d\dot{m}_s}{d\omega}$), (f) slope of moisture content variation ($\frac{d\dot{\omega}}{d\omega}$).

experiments ($\mathbf{Y_{des}}$) during the training phase (80 %, 166 samples). A notable resemblance between the $\mathbf{Y_{ob}}$ and $\mathbf{Y_{des}}$ outputs is observed, indicating effective network training, as illustrated in Fig. 4 and described in Table 2. Consequently, the ANN is now capable of estimating data (such as drying speed) for samples that were not part of the training process. An automated model has been developed to estimate drying speed based on new sets of input data (air speed (m/s), air temperature (°C), relative humidity (%), chip column height (cm) y average sliver length (m)).

Fig. 5 presents the results of the network validation phase for 41 samples (20 %) of the input data that were not part of the training, with the desired and obtained output values. Again, there is a similarity between the outputs, proving the effectiveness of the model created via ANN. The MSE between outputs for this phase was 0.000996, below the specified value.

Fig. 6 shows the behavior of the average relative drying speed (g/s kg) ($\overline{\dot{m}_w}$) y average absolute drying speed (g/s) ($\overline{\dot{m}_s}$) as a function of air velocity (m/s), air temperature (°C), and relative humidity (%). It is observed that, for the attribute $\overline{\dot{m}_s}$, the factors (air velocity (m/s), air temperature (°C), and relative humidity (%)) had no significant impact. However, for the $\overline{\dot{m}_w}$, the air temperature and relative humidity exhibited the expected responses, with higher values of $\overline{\dot{m}_w}$ observed at low humidity and high temperatures. In this case, air velocity did not influence the $\overline{\dot{m}_w}$, presenting the same results for the desired one.

Fig. 7 shows as an example the results of two drying experiments carried out with the experimental device. Some researchers have already described the dependence of the drying speed on moisture content. Research such as Berberović & Milota (2011) [25] or Moufakkir et al. (2019) [26] reported that the drying speed changes with biomass moisture content. When the mass represents high moisture content values the drying speed is constant, but from a critical moisture content the drying speed begins to decrease linearly [27]. Subsequently, the drying speed is modified in a non-linear way. This is also observed in our results. The critical moisture content in the experiments shown is around 42 %. However, very different curves are observed, and whose prediction has been unsuccessful, before the appearance of artificial intelligence.

The results obtained through neural networks allow us to predict the average drying speed of any process using air temperature, air speed and relative air humidity data as input. This represents a technical advance.

Table 4 shows the values of the weights applied to each of the signals transmitted between two neurons. Table 5 shows the bias values applied to each of the neurons.

When the mass transfer coefficients (h_m) obtained experimentally are

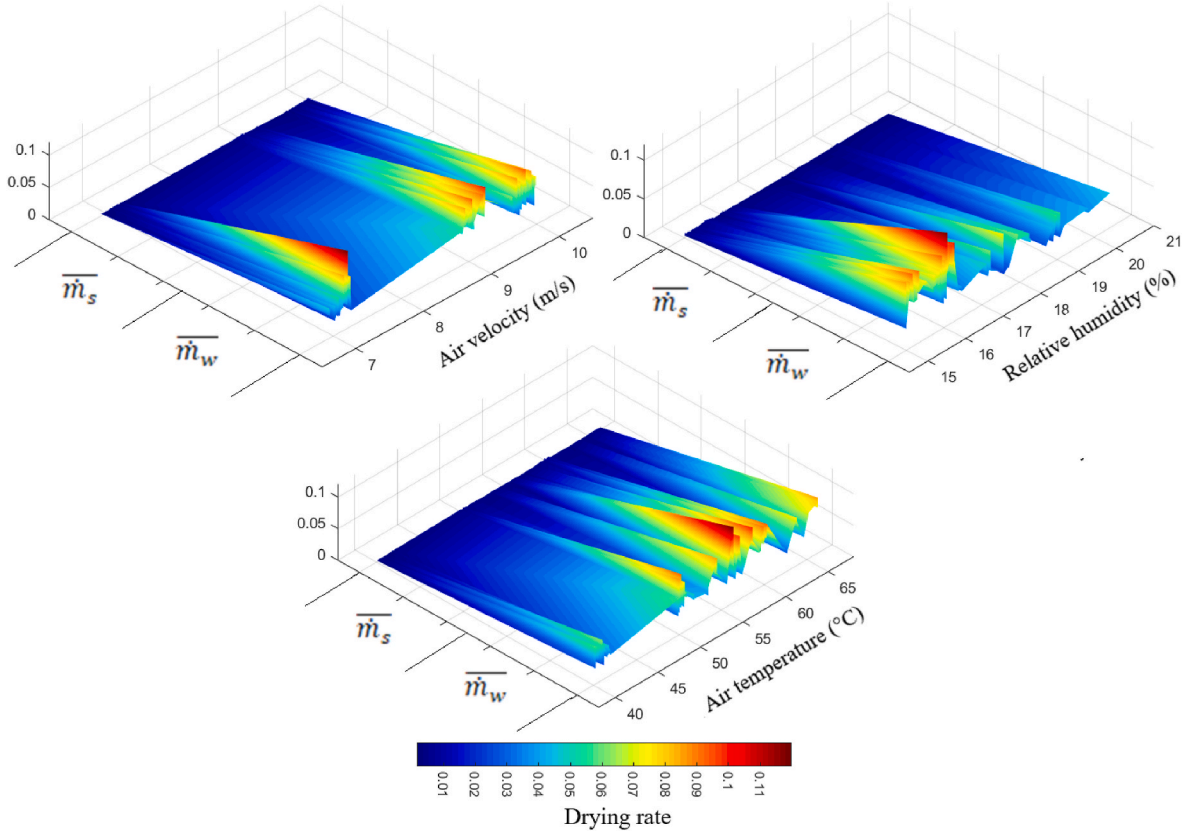

Fig. 6. Average relative drying speed (g/s kg) ($\overline{\dot{m}_w}$) y average absolute drying speed (g/s) ($\overline{\dot{m}_s}$) as a function of air speed (m/s), air temperature (°C) y relative humidity (%), obtained via ANN.

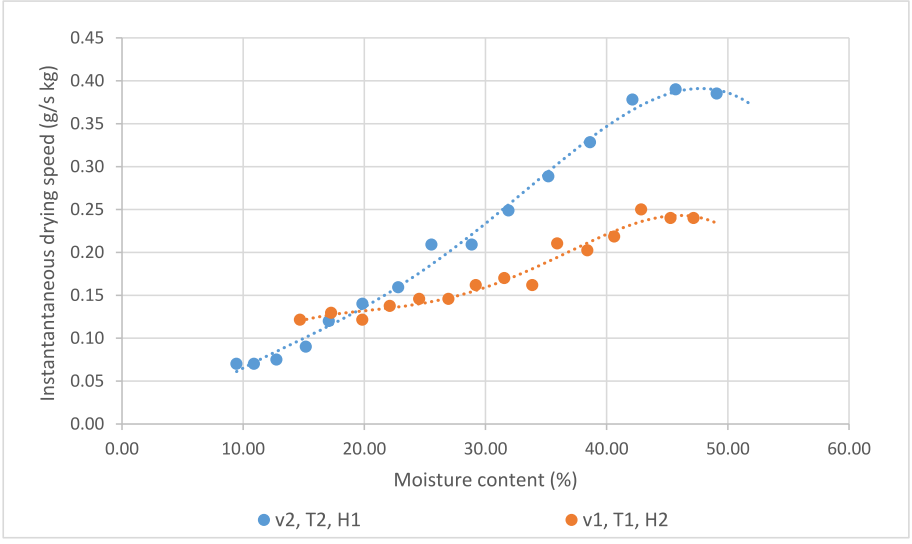

Fig. 7. Representation of the relative drying speed (a) speed v_2, Temperature T_3, height H_1; (b) air speed v_1, Temperature T_1, height H_2.

compared with those calculated from the Sherwood number, it is observed that predictions based on mass transfer models overestimate their value (see Table 6). In Fig. 8 you can see the density functions of the normal distribution obtained for the experimental and theoretical data. The experimental h_m present values 30 times lower than those obtained through equation (7). On the other hand, the experimental variability of these coefficients is much greater than that obtained from calculations based on mass transfer models (Fig. 9).

The theoretical models to calculate the mass transfer coefficient by convection do not present significant variations for the air circulation conditions that we have taken for our experimentation (temperatures T_1, T_2 and T_3, speed v_1 and v_2, height H_1 and H_2). The mean value of h_m has been 0.075 m kg^{-1} s^{-1} and standard deviation of 0.005 m kg^{-1} s^{-1}. However, it can be observed that in the experiments the variations of h_m are large, with a mean of 0.0025 m kg^{-1} s^{-1} and a standard deviation of 0.0008 m kg^{-1} s^{-1}. Despite being able to establish regression models that relate the theoretical values and values of the experimental results for the calculation of the average drying speed, the use of neural

Table 4
Weights of the connections between the neurons of the hidden layer and the output layer (w_{mi}).

		Neurons output layer					
		i_1	i_2	i_3	i_4	i_5	i_6
Neurons hidden layer	$\mathbf{m_1}$	−0.3075	−0.2041	−0.1034	−0.3378	−0.2017	−0.0731
	$\mathbf{m_2}$	0.4915	0.2081	0.9887	0.0067	−0.1812	−0.6103
	$\mathbf{m_3}$	−0.0605	0.0585	0.2085	0.1464	0.4329	1.6707
	$\mathbf{m_4}$	0.2186	0.6598	0.0034	0.2624	0.8173	0.1504
	$\mathbf{m_5}$	0.4855	0.3939	0.1884	0.4210	0.2279	−1.0281
	$\mathbf{m_6}$	0.4114	0.4800	0.3876	0.5174	0.6223	0.0236
	$\mathbf{m_7}$	0.3375	0.2889	0.5598	0.3983	0.3297	−0.0590
	$\mathbf{m_8}$	−0.5656	−0.4771	−0.3403	−0.6351	−0.4563	0.4676
	$\mathbf{m_9}$	−0.3957	0.2054	−0.4577	0.0254	0.5464	0.7869
	$\mathbf{m_{10}}$	−0.6689	−0.5166	−0.6632	−0.3608	−0.3205	−0.8750

Table 5
Bias of the neurons of each layer (hidden and output).

	Neurons hidden layer (m_x1)		Neurons output layer (i_x1)
1	−1.6501	**1**	−0.64487
2	−2.1719		
3	−1.3691	**2**	−1.1961
4	1.7207		
5	0.15466	**3**	0.29697
6	−0.27355		
7	−0.50961	**4**	−1.002
8	−0.058954		
9	1.0268	**5**	−1.2991
10	−2.0311	**6**	−1.3135

Table 6
Comparison coefficient of convection mass transfer.

	Theorical h_m	*Experimental* h_m	*Theorical* h_m / *Experimental* h_m
Count	219	219	219
Average	0,075	0,0025	28,4219
Standard deviation	0,005	0,0008	10,1592
Coefficient of variation	11,34 %	36,57 %	35,74 %
Minimum	0,052	0,0012	12,91
Maximum	0,099	0,0058	55,76
Range	0,047	0,004	42,85
Standardized Bias	0,217	1,03	1,71
Standardized Kurtosis	−0,317	−0,71	−0,067

networks allows us adjustments that are capable of predicting these variations and, therefore, being able to predict drying speed much more efficiently.

In the comparative study between traditional mass transfer models and experimental data in drying processes, a significant discrepancy in the estimation of the convection coefficient has been highlighted. It has been observed that the values obtained from the Sherwood number tend to overestimate said coefficient. This overestimation is of particular importance in the case of the application of these models to porous materials such as wood.

It has been identified that the convection coefficient applied to wood is approximately 30 times lower than the value calculated from traditional models. This substantial discrepancy is attributed to the influence of capillary phenomena and electrostatic forces present between the material and the water particles during the drying process.

In the context of mass transfer, porous materials such as wood exhibit particular behaviors due to their microscopic structure and physical properties. The presence of interconnected pores facilitates the migration of water through the material, but also introduces complications in the estimation of mass transfer coefficients.

Capillary forces within the pores of wood influence the rate of evaporation and therefore mass transfer. These forces can trap water within the pores, slowing the drying process compared to non-porous materials. Furthermore, electrostatic forces between the material and water can also influence the distribution and movement of the liquid during the drying process.

Therefore, it is crucial to consider these specific characteristics of porous materials when applying mass transfer models in drying processes, especially in the case of wood, where discrepancies between estimated values and experimental data can be significant. Furthermore, the use of other tools such as Convolutional Neural Networks (CNN), which are effective in analyzing detailed images of the porous structure of materials, provides a deeper understanding of their impact on drying processes. Similarly, Recurrent Neural Networks (RNN) are valuable for modeling data related to the drying of various materials and capturing the complex interactions between variables involved in this process. These advanced machine learning techniques have the potential to provide deeper insights into biomass drying processes and other porous

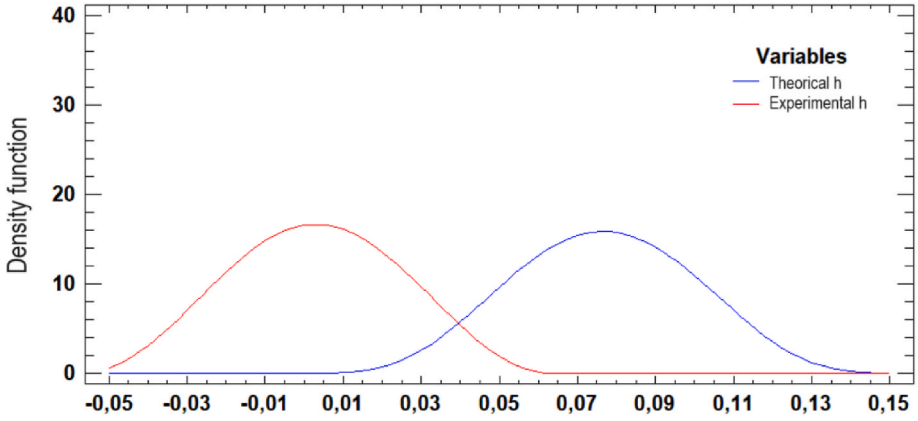

Fig. 8. Density function of the mass transfer coefficient based on the data obtained in the experiments and from the theoretical model.

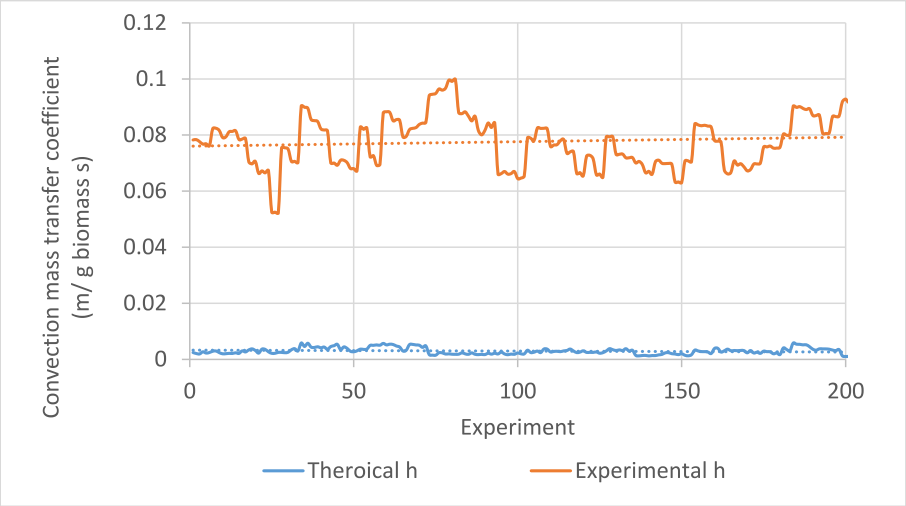

Fig. 9. Comparison of the convection mass transfer coefficients obtained in the experiments and through the theoretical model.

materials, and can help mitigate discrepancies between theoretical estimates and experimental results, considering the particularities of these materials.

4. Conclusions

The study findings indicate a clear correlation between drying rate and moisture content in biomass, consistent with previous research. Moreover, they introduce a novel approach utilizing neural networks to predict drying speed accurately based on input variables such as air temperature, air speed, and relative air humidity. This development is significant for enhancing the predictability and control of drying processes.

Specifically, the study identifies an effective neural network architecture comprising an input layer of six neurons followed by a hidden layer of 10 neurons. This configuration yields satisfactory results in predicting average drying speed (Mean absolute drying speed, Mean relative drying speed, coefficient of mass transfer). Also it allow calculate de variation of these values according the material moisture content. The study also provides detailed information regarding the weights assigned to each signal transmitted between neurons within the network, as well as the biases applied to individual neurons. These insights are crucial for understanding the precise functioning and configuration of the neural network within the context of this study.

The mass transfer coefficient is overestimated when it is calculated through the Sherwood number. In wood chips the neural network allows more accurate predictions with little error compared to experimental data.

A challenge for future research is, instead of obtaining the average drying values, to obtain the plot of the drying curves based on the air temperature, relative humidity of the air, air speed, characteristic length of the pieces and species of wood from neural networks. Our next work will focus on this objective.

CRediT authorship contribution statement

Borja Velázquez Martí: Writing – review & editing, Resources, Project administration, Methodology, Investigation, Funding acquisition, Formal analysis, Data curation, Conceptualization. **Alfredo Bonini Neto:** Writing – original draft, Software, Methodology, Investigation. **Daniel Nuñez Retana:** Writing – original draft, Investigation. **Artemio Carrillo Parra:** Resources, Investigation, Funding acquisition. **Sebastian Guerrero-Luzuriaga:** Investigation.

Data availability

Data will be made available on request.

References

[1] R.P. Ramachandran, M. Akbarzadeh, J. Paliwal, S. Cenkowski, Computational fluid dynamics in drying process modelling—a technical review, Food Bioprocess Technol. 11 (2018) 271–292.
[2] X. Wang, B. Qin, H. Xu, W. Zhu, Rotary drying process modeling and online compensation, Control Eng. Pract. 41 (2015) 38–46.
[3] N. Malekjani, S.M. Jafari, Simulation of food drying processes by Computational Fluid Dynamics (CFD); recent advances and approaches, Trends Food Sci. Technol. 78 (2018) 206–223.
[4] I.C. Kemp, D.E. Oakley, Modelling of particulate drying in theory and practice, Dry. Technol. 20 (2002) 1699–1750.
[5] I. Dincer, A.Z. Sahin, A new model for thermodynamic analysis of a drying process, Int. J. Heat Mass Tran. 47 (2004) 645–652.
[6] R.O. Lamidi, L. Jiang, P.B. Pathare, Y. Wang, A.P. Roskilly, Recent advances in sustainable drying of agricultural produce: a review, Appl. Energy 233 (2019) 367–385.
[7] J. Yi, X. Li, J. He, X. Duan, Drying efficiency and product quality of biomass drying: a review, Dry. Technol. 38 (2020) 2039–2054.
[8] C. Di Blasi, Simultaneous heat, mass and momentum transfer during biomass drying, Dev. Thermochem. Biomass Conv. 2 (1997) 117–131. Volume 1.
[9] Z. Erbay, F. Icier, A review of thin layer drying of foods: theory, modeling, and experimental results, Crit. Rev. Food Sci. Nutr. 50 (2010) 441–464.
[10] J. Han, Y. Choi, J. Kim, Development of the process model and optimal drying conditions of biomass power plants, ACS Omega 5 (2020) 2811–2818.
[11] S. Buzrul, Reassessment of thin-layer drying models for foods: a critical short communication, Processes 10 (1) (2022) 118.
[12] C. Ertekin, M.Z. Firat, A comprehensive review of thin-layer drying models used in agricultural products, Crit. Rev. Food Sci. Nutr. 57 (2017) 701–717.
[13] A.M. Castro, E.Y. Mayorga, F.L. Moreno, Mathematical modelling of convective drying of fruits: a review, J. Food Eng. 223 (2018) 152–167.
[14] Y. Zhu, P. Wang, D. Sun, Z. Qu, B. Yu, Multiphase porous media model with thermo-hydro and mechanical bidirectional coupling for food convective drying, Int. J. Heat Mass Tran. 175 (2021) 121356.
[15] R. Moreno-Muñoz, G. Antolín-Giraldo, A. Reyes-Salinas, Experimental Investigation on Drying of Forest Biomass Particles in a Mechanically Stirred Fluidized Bed, 2023.
[16] M. Omid, A. Baharlooei, H. Ahmadi, Modeling drying kinetics of pistachio nuts with multilayer feed-forward neural network, Dry. Technol. 27 (2009) 1069–1077.
[17] A. Moreira, A. Bonini Neto, C. dos S. Batista Bonini, L.A.C. Moraes, R. Heinrichs, Prediction of soybean yield cultivated under subtropical conditions using artificial neural networks, Agron. J. 115 (2023) 1981–1991.
[18] A. Bonini Neto, A. Moreira, C. dos Santos Batista Bonini, M. Campos, C. Andrighetto, Fuzzy logic and artificial neural network Perceptron multi-layer and radial basis in estimating marandu grass yield in integrated systems, Commun. Soil Sci. Plant Anal. 54 (2023) 2965–2976.
[19] A.V. de Souza, A. Bonini Neto, J.C. Piazentin, B.J.D. Junior, E.P. Gomes, C. dos S. B. Bonini, F.F. Putti, Artificial neural network modelling in the prediction of bananas' harvest, Sci. Hortic. 257 (2019) 108724.
[20] D. Wang, M. Zhang, A.S. Mujumdar, D. Yu, Advanced detection techniques using artificial intelligence in processing of berries, Food Eng. Rev. (2022) 1–24.

[21] M. Aghbashlo, S. Hosseinpour, A.S. Mujumdar, Application of artificial neural networks (ANNs) in drying technology: a comprehensive review, Dry. Technol. 33 (2015) 1397–1462.
[22] AENOR, UNE-EN 17225-4, Solid biofuels - fuel specifications and classes - Part 4: graded wood chips (ISO 17225-4:2021). https://tienda.aenor.com/norma-une-en-iso-18134-3-2024-n0072517, 2021. (Accessed 12 February 2024).
[23] AENOR, Solid biofuels - determination of moisture content - Part 3: moisture in general analysis sample (ISO 18134-3:2023). https://tienda.aenor.com/norma-une-en-iso-18134-3-2024-n0072517, 2024. (Accessed 12 February 2024).
[24] Matlab, Mathworks, 2023. http://www.mathworks.com. (Accessed 11 February 2024).
[25] A. Berberović, M.R. Milota, Impact of wood variability on the drying rate at different moisture content levels, For. Prod. J. 61 (2011) 435–442.
[26] A. Moufakkir, A. Elbouzidi, A. Samaouali, Curves characteristic of natural drying of five species of wood, Adv. Stud. Theor. Phys. 13 (2019) 55–66.
[27] G. Erber, J. Routa, M. Kolstrom, C. Kanzian, L. Sikanen, K. Stampfer, Comparing two different approaches in modeling small diameter energy wood drying in logwood piles, Croat. J. For. Eng.: J. Theory Appl. For. Eng. 35 (2014) 15–22.